ORGANOMETALLICS

Article

Cite This: *Organometallics* 2019, 38, 2758−2769

pubs.acs.org/Organometallics

A Family of Cross-Conjugated Polyenynes Capped by Co^{III}(cyclam): Syntheses, Molecular and Electronic Structures

Sean N. Natoli,*[,†,‡] Matthias Zeller,[‡] and Tong Ren*[,‡]

[†]Department of Chemistry, University of California, Berkeley, California 94720, United States

[‡]Department of Chemistry, Purdue University, West Lafayette, Indiana 47907, United States

Supporting Information

ABSTRACT: Transition-metal complexes bridged by acyclic cross-conjugated frameworks are uncommon and can possess structurally unique nonlinear topologies and intriguing electron transport properties. Herein, we report the attachment of extended enyne scaffolds, L1 (3,6-diethynyl-2,7-dimethylocta-2,6-dien-4-yne) and L2 (5-ethynyl-6-methylhepta-5-en-1,3-diyne), to a Co^{III}(cyclam) unit. Mononuclear complexes **Co-L1** ([Co(cyclam)(L1)Cl]PF_6) and **Co-L2** ([Co(cyclam)(L2)Cl]-PF_6) were synthesized in modest to good yields under methanolic weak-base conditions. Similarly, bimetallic compounds **Co-L1-Co** ([{Co(cyclam)Cl}$_2$ (μ-L1)]$(PF_6)_2$) and **Co-L2-Co** ([{Co-(cyclam)Cl}$_2$(μ-L2)]$(PF_6)_2$) were prepared in modest yields from the reaction of [Co(cyclam)Cl_2]Cl with **Co-L1** or **Co-L2**, respectively. Alternatively, **Co-L1-Co** and **Co-L2-Co** were prepared directly from L1 and L2 in the presence of excess [Co(cyclam)Cl_2]Cl. Oxidative coupling of **Co-L1** and **Co-L2** yielded the respective dimeric complexes {**Co-L1-**}$_2$ ([{Co(cyclam)Cl}$_2$(μ-(L1)$_2$)]$(PF_6)_2$) and {**Co-L2-**}$_2$ [{Co(cyclam)Cl}$_2$(μ-(L2)$_2$)]$(PF_6)_2$) in modest yields. Both {**Co-L2-**}$_2$ (C14) and {**Co-L1-**}$_2$ (C16) are examples of the longest bridged transition-metal enyne complexes and bridged Co^{III}(cyclam) complexes to date. {**Co-L1-**}$_2$ crystallized in a unique *s*-cis−trans−cis orientation that is stabilized by a close intermolecular $\pi-\pi$ interaction. Cyclic voltammetry measurements of cobalt-L1 and -L2 complexes revealed isolated Co^{III}(cyclam) units, where redox potentials were determined by structural characteristics prior to the first intervening olefin. In contrast to the cases of shorter enyne bridged Co^{III}(cyclam) complexes (≤5 carbons), the LUMOs from DFT analysis do not display orbital mixing spanning the entirety of the enyne framework. This work highlights the diversity in structural and electronic properties obtained with transition-metal enyne frameworks. Such complexes are intriguing as nonlinear moieties for supramolecular assemblies and as long-range molecular insulators or switches.

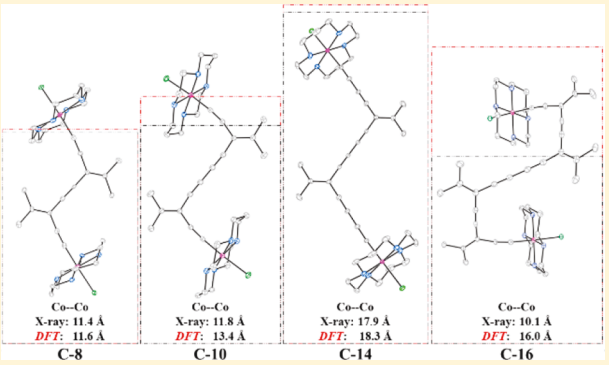

INTRODUCTION

Conjugated organic alkynes and metal alkynyls remain intensely pursued targets for electronic and optoelectronic materials.[1−6] Linear metal alkynyls, especially those based on metal-oligoynyls, are attractive prototypes for molecular wires,[7−10] and active materials for molecular devices.[11−13] In comparison to the corresponding linear systems, cross-conjugated organic and metal alkynyls have received less attention from a materials perspective. It is noteworthy that Ratner and co-workers proposed that electronic conductance switching, with a substantial dynamic range, may be realized with rigid molecules containing a *geminal* diethynylethene (*gem*-DEE) unit based on computational studies.[14,15] Building on the protocols developed by Diederich and Tykwinski,[16−21] a number of laboratories including ours have explored metal compounds containing *gem*-DEE or related ligands.[22] Earlier on, our laboratory succeeded in preparing 3-(dibromomethylidene)-1,5-bis(ferrocenyl)penta-1,4-diyne from 1,5-bis(ferrocenyl)penta-1,4-diyn-3-one via a Corey−Fuchs olefination reaction.[23] The *gem*-DEE type ligands were used in both a monodentate fashion in the formation of *trans*-Ru_2(DMBA)$_4$(*gem*-DEE-Ar) (DMBA = *N*,*N*′-dimethylbenzamidinate)[24] and in a bridging fashion, as in the synthesis of [Ru_2(*ap*)$_4$]$_2$(μ-*C*,*C*-*gem*-DEE) (*ap* = 2-aniliopyridinate).[25] Though the stepwise one-electron reductions with a ΔE = 160 mV was revealed in the cyclic voltammogram (CV) of the latter compound, the electronic coupling between two Ru_2(*ap*)$_4$ units mediated by *gem*-DEE was deemed weak through spectroelectrochemical study.[25] Bruce and co-workers reported the reaction between Cp*Ru(dppe)(C≡CH) (dppe = 1,2-bis(diphenylphosphino)ethane) and oxalyl chloride affording [{Ru(dppe)Cp*}C≡C]$_2$(CO), which was converted subsequently to the [{Ru(dppe)Cp*}C≡C]$_2$(C═C(CN)$_2$) derivative.[26] Stepwise one-electron oxidations of Ru^{II} centers with significant ΔEs (ca. 200 mV) were observed for these complexes, though further assessment of Ru−Ru electronic coupling was not performed.[26] Fan and co-workers reported

Received: May 12, 2019
Published: June 27, 2019

DOI: 10.1021/acs.organomet.9b00313
Organometallics 2019, 38, 2758−2769

Scheme 1. Syntheses of L1, L2, Co-L1, and Co-L2[a]

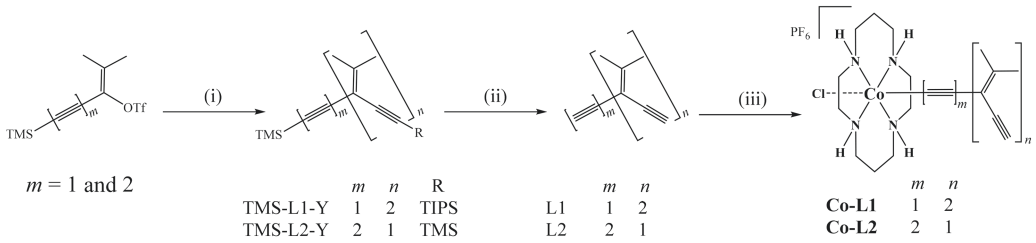

[a]Conditions: (i) *gem*-diethynylethane or trimethylsilylacetylene, $Pd(Cl_2)_2(PPh_3)_2$, CuI, THF, Et_2NH, rt, 24 h; (ii) TBAF, THF, rt; (iii) $[Co(cyclam)Cl_2]Cl$, Et_3N, MeOH, reflux, 16−40 h, then $NaPF_6$(aq).

Scheme 2. Syntheses of Compounds Co-L1-Co, Co-L2-Co, {Co-L1-}$_2$, and {Co-L2-}$_2$[a]

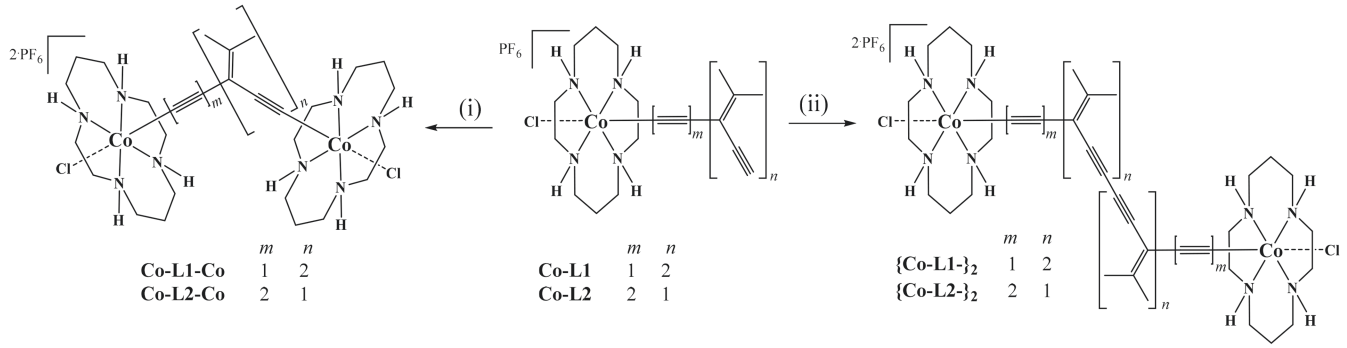

[a]Conditions: (i) 1.2 equiv $[Co(cyclam)Cl_2]Cl$, Et_3N, MeOH, reflux 16 h; (ii) CuCl/TMEDA (cat.), O_2, MeOH, 6 h.

two series of bis(ferrocene) bridged by *gem*-DEE, one based on xanthene and its analogues,[27] and the other based on cyclohexyl and its analogues,[28] and elucidated a Robin-Day class II mixed valency for the (Fc−Fc$^+$) ions in these compounds. With the cross-conjugated $Ph_2C{=}C(C{\equiv}CH)_2$ ligand. Low and co-workers prepared both the monocapped $CpRu(PPh_3)_2$ complex and the bridged bis(ferrocenyl) complex, and the Fc−Fc interactions in the latter were probed using IR spectroelectrochemistry.[29] Subsequently, Low, Lapinte and co-workers prepared bimetallic M(dppe)Cp* (M = Ru and Fe) complexes bridged by 1,1-bis(alkynyl)-2-ferrocenylethene and probed the mixed valency using both vis−NIR and IR spectroelectrochemistry.[30] More recently, several dinuclear uranium complexes bridged by 1,3-diethynylbenzene have been prepared and structurally characterized, expanding the scope of cross-conjugated organometallics with the inclusion of actinide complexes.[31] In a separate yet related study, Liu and co-workers investigated the quantum interference effect in several dimers of quadruply bonded Mo_2 with a *meta*-phenylene unit (*cross conjugated*) in the bridge.[32]

In an effort to develop metal alkynyl chemistry based on more sustainable materials, our interest has shifted toward 3*d* metal complexes supported by polyaza macrocycles, especially cyclam and its *C*-substituted analogues.[33,34] Early work revealed the feasibility of synthesizing early transition-metal *gem*-DEE complexes with the preparation of *trans*-[M(cyclam)-(*gem*-DEE)$_2$], where M is Cr^{III},[24] or Fe^{III}.[35,36] More extensive efforts toward Co^{III} species demonstrated the attainability of [M-(*μ*-*gem*-DEE)-M], in addition to the *trans*-[Co(cyclam)-(*gem*-DEE)(C$_2$R)] type complexes, and crystal structures of [Co(cyclam)-(*μ*-*gem*-DEE)-Co(cyclam)] and [Co(cyclam)-(*μ*-(*gem*-DEE)$_2$)-Co(cyclam)] were the first structurally characterized bimetallic species with *gem*-DEE bridges.[37,38] In this contribution, we have further expanded this exploration to the preparation of Co^{III}(cyclam) complexes based on extended enyne scaffolds (Schemes 1 and 2 below), and investigated their structural, voltammetric, and spectroscopic properties with elaboration of molecular and electronic structures via DFT calculations.

RESULTS AND DISCUSSION

Syntheses. A series of polyenyne scaffolds can be readily prepared from the coupling of vinyl triflates and acetylenes under Sonogashira cross-coupling conditions.[17] This procedure gave triisopropyl(7-methyl-3-(propan-2-ylidene)-6-((trimethylsilyl)ethynyl)octa-6-en-1,4-diyn-1-yl)silane (TMS-triethynyldiethene; TMS-L1) and triisopropyl(3-(propan-2-ylidene)-7-(trimethylsilyl)hepta-1,4,6-triyn-1-yl)silane (TMS-butadiynylethenylethene; TMS-L2) in yields up to 82% and 93%, respectively (Scheme 1).[18,39] In their silyl capped form, both TMS-L1 and TMS-L2 were stable for multiple weeks when stored at −20 °C. Desilylation was accomplished using tetrabutylammonium fluoride (TBAF) in a dilute solution of THF. However, faster degradation was observed for the free ethynyl ligands upon standing. Therefore, desilylation was performed immediately before metalation, and ligands were used directly following an ethereal extraction without further purification.

Similar to the preparation of [Co(cyclam)(*gem*-DEE)Cl]$^+$,[38] a methanolic suspension of $[Co(cyclam)Cl_2]Cl$ was refluxed with a slight excess of L1 in the presence of Et_3N to yield $[Co(cyclam)(L1)Cl]PF_6$ (**Co-L1**) as an orange crystalline material in 76% yield after purification and counterion exchange (Scheme 1).[40] Time course mass spectrometric analysis indicated that all of the $[Co(cyclam)Cl_2]Cl$ starting

DOI: 10.1021/acs.organomet.9b00313
Organometallics 2019, 38, 2758−2769

material was consumed after 16 h. However, when the same conditions were employed to synthesize the unsymmetrical enyne [Co(cyclam)(L2)Cl]PF_6 (**Co-L2**), NMR and electrochemical measurements revealed a mixture of alkynyl-cobalt bound species after 16 h, namely, the ethynyl-(Co—C≡C—$C(C_3H_6)$—C≡C—C≡C—H) and butadiynyl-(Co—C≡C—C≡C—$C(C_3H_6)$—C≡C—H) bound compounds (Figure S7). This result was unexpected, as the butadiynyl fragment is more activated toward metal−carbon bond formation and sterically less-demanding than the alternative ethynyl linkage. Diruthenium complexes bearing an L2 fragment were reported, and their synthesis required a silyl protecting group to prevent similar alkynyl scrambling.[41] Therefore, preliminary work to yield **Co-L2** required additional synthetic steps starting from the reaction of [Co(cyclam)Cl_2]Cl with the TIPS-L2 ligand, followed by desilylation with TBAF. Fortunately, extending the reflux time to 40 h resulted in only the butadiynyl-bound form of **Co-L2** in an isolated yield of 41%. This result suggests that there might be some reversibility in metal-alkynyl binding under these conditions or the continuous degradation of the less-stable ethynyl-bound compound.

A dicobalt complex with L1 as the bridging ligand [{Co(cyclam)Cl}$_2$(μ-L1)]$(PF_6)_2$ (**Co-L1-Co**) was obtained in a yield of 78% by refluxing **Co-L1** with 1.2 equiv of [Co(cyclam)Cl_2]Cl under weak base conditions (Scheme 2). Alternatively, **Co-L1-Co** could be obtained directly from the reaction of L1 with 2.2 equiv of [Co(cyclam)Cl_2]Cl, which led to **Co-L1-Co** in an isolated yield of 56% yield. Similarly, the reaction of **Co-L2** with excess [Co(cyclam)Cl_2]Cl yielded the binuclear complexes [{Co(cyclam)Cl}$_2$(μ-L2)]$(PF_6)_2$ (**Co-L2-Co**) as a red powder (64% based on **Co-L2**). Overall yield was improved by refluxing **L2** directly with 2.2 equiv of [Co(cyclam)Cl_2]Cl to give **Co-L2-Co** in an isolated yield of 60% (based on cobalt).

It has previously been demonstrated that Glazer coupling under Hay conditions is a convenient method to yield dimeric transition metal constructs {M—C≡C—}$_2$ from the free ethynyl mononuclear {M—C≡C—H} compounds.[42,43] Reports on oligoynyl Co^{III}(cyclam) compounds, using a similar protocol, yielded elongated unsaturated carbon bridge lengths of up to 12 carbons (C12). However, this compound suffered from rapid degradation and low synthetic yields (≤11%).[40] Fortunately, the unsaturated enyne scaffolds proved more amenable to Glazer coupling, and the 14 carbon (C14) bridged dimeric compound [{Co(cyclam)Cl}$_2$(μ-(L2)$_2$)]$(PF_6)_2$ {**Co-L2-**}$_2$ was obtained in yields up to 33% (Scheme 2). Furthermore, the 16 carbon (C16) bridged dimeric compound [{Co(cyclam)Cl}$_2$(μ-(L1)$_2$)]$(PF_6)_2$ {**Co-L1-**}$_2$ was synthesized from the oxidative homocoupling of **Co-L1** in an isolated yield of 24%. However, the monomeric [Co(cyclam)({L2}$_2$)-Cl]$^+$ complex was found to be too unstable for complete characterization, and a subsequent coupling reaction did not yield the longer oligomer [{Co(Cl)}$_2$(μ-({L2}$_4$))]$^{2+}$.

All reported Co^{III} compounds are diamagnetic and were fully characterized by ESI-MS, ^{1}H NMR, IR, elemental analysis, and single crystal X-ray diffraction analysis. Mono- (**Co-L1** and **Co-L2**) and bimetallic (**Co-L1-Co** and **Co-L2-Co**) compounds were stable for several months at −20 °C. Dimeric compounds ({**Co-L1-**}$_2$ and {**Co-L2-**}$_2$) were stable for multiple weeks at −20 °C. Though complexes with chloride as the counterion were obtained in high purity,[40,44] they have limited solubility in organic solvents. For consistency, all analyses were performed and reported with PF_6^- as the counterion.

Absorption Spectroscopy. Electronic absorption spectra were taken in acetonitrile for cobalt-L1 and -L2 complexes and are reported in Figures 1 and 2, respectively. Absorption

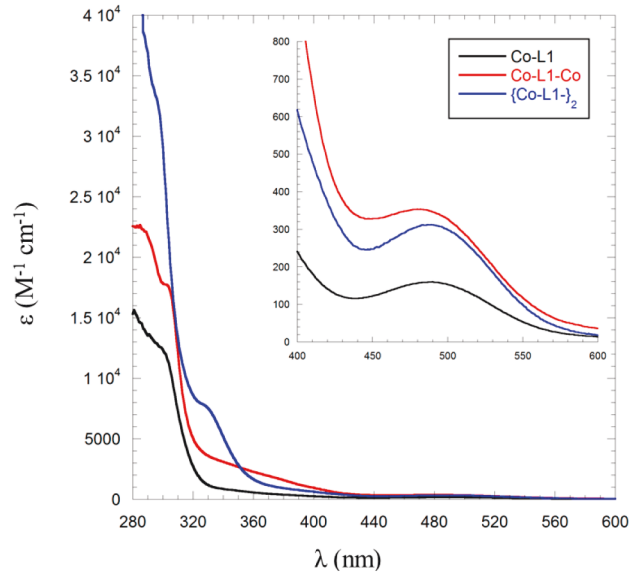

Figure 1. Absorption spectrum of **Co-L1** (black), **Co-L1-Co** (red), and {**Co-L1-**}$_2$ (blue) in MeCN with the inset showing the metal-based *d*−*d* transition.

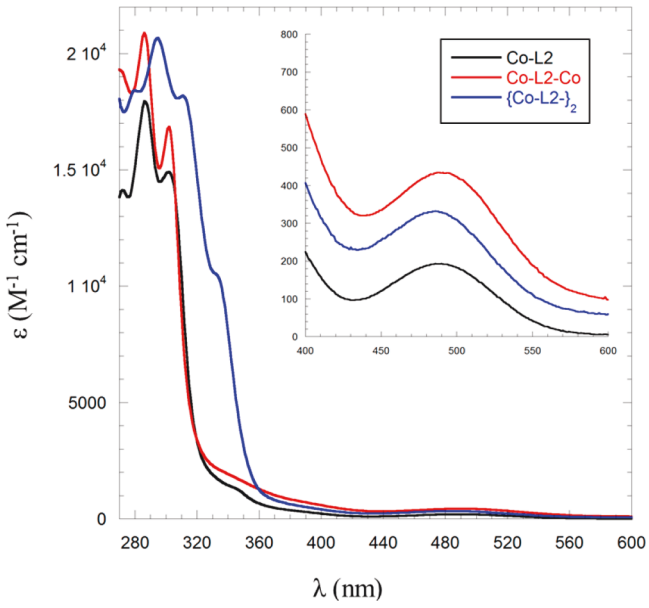

Figure 2. Absorption spectrum of **Co-L2** (black), **Co-L2-Co** (red), and {**Co-L2-**}$_2$ (blue) in MeCN with the inset showing the metal-based *d*−*d* transition.

spectra of metal free cross-conjugated isopolytriacetylenes, isopolydiacetylenes, and related oligoenynes were previously surveyed for their π-electronic properties.[18,45] For the constructs reported herein, the ultraviolet absorption spectra are dominated by absorptions corresponding to the enyne scaffold. In the case of the L2 frameworks, these absorptions are highly structured, similar to what is observed for bis(trimethylsilyl)butadiyne.[46] Contrary to the L2 series, the

DOI: 10.1021/acs.organomet.9b00313
Organometallics 2019, 38, 2758−2769

ultraviolet absorption spectra for the L1 frameworks are not structured. These trends are akin to those reported for their metal-free analogues.[18,45] A slight red shift in the λ_{max} (≤21 nm) values is observed across the L2 series as conjugation length increases. Shifts of similar magnitude were observed for silyl capped iso-PDAs and were surmised to indicate weak electronic delocalization.[18] No significant change in λ_{max} values were noticed for L1 compounds. In general, the addition of the Co^{III}(cyclam) unit does not distort or dampen the cross-conjugated properties of the reported enyne frameworks.

All of the Co^{III} complexes were isolated as red to red-orange colored materials, with color arising from a $d-d$ transition ($^1A_{1g}$ to $^1T_{1g}$) between 486 and 490 nm. The narrow range of $d-d$ λ_{max} observed for the Co^{III}(cyclam) systems investigated here is unique, as other Co^{III}(cyclam) systems including those of oligoyn-diyl frameworks had spectral shifts up to 20 nm upon oligomerization[40] or addition of $[Co(cyclam)Cl]^{2+}$ units.[44] Surprisingly, only a small shift in λ_{max} is observed across the two series, with the greatest change being 9 nm between **Co-L1-Co** and **Co-L1**. The consistency in λ_{max} values suggests that the cobalt centers in the reported complexes are in a nearly identical ligand field regardless of the enyne structural composition beyond the closest intervening olefin.

Molecular Structures. The molecular structures of **Co-L1**, **Co-L1-Co**, {**Co-L1-**}$_2$, and {**Co-L2-**}$_2$ have been established by single crystal X-ray diffraction studies. X-ray quality crystals were obtained through slow diffusion of diethyl ether into a concentrated methanolic solution (**Co-L1**, **Co-L1-Co**, and {**Co-L2-**}$_2$) or acetonitrile solution ({**Co-L1-**}$_2$). The structures of the monomeric complex **Co-L1**, the bimetallic complex **Co-L1-Co**, and the dimeric complexes {**Co-L1-**}$_2$ and {**Co-L2-**}$_2$ are represented in Figures 3–6, respectively.

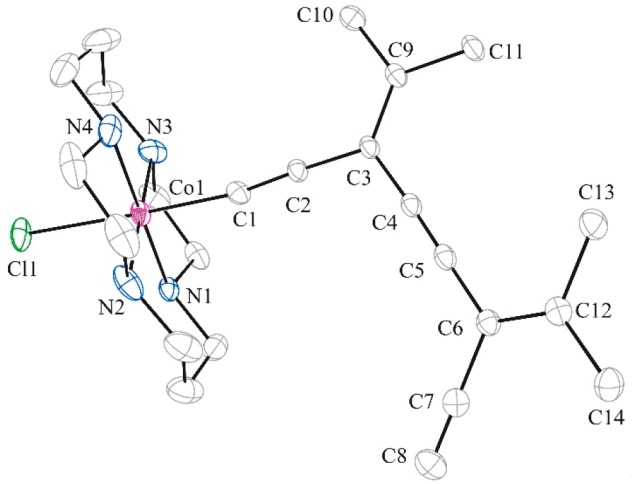

Figure 3. Molecular plot of [**Co-L1**]$^+$ at 30% probability level. Hydrogen atoms, solvent molecules, and counterion were omitted for clarity.

Relevant bond lengths and angles are reported in Table 1. Experimental crystallographic data are provided in the Supporting Information, and the data were deposited, in CIF format, with the CCDC database.

The monomeric complex **Co-L1** has an octahedral geometry, where the secondary amines of cyclam, in a trans-III configuration, lie in the equatorial plane about the Co^{III} ion. The Cl–Co–C1 bond angle is nearly linear, and the **L1** scaffold crystallized in a rarely observed *s*-cis orientation.[39,44]

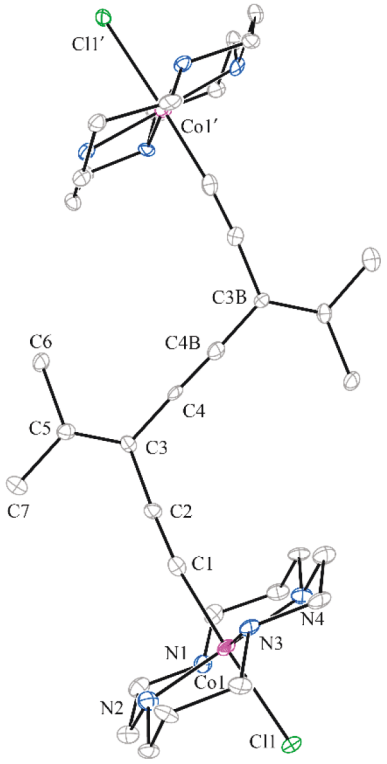

Figure 4. Molecular plot of [**Co-L1-Co**]$^{2+}$ at 30% probability level. Hydrogen atoms, solvent molecules, and counterion were omitted for clarity.

This *s*-cis orientation results in a significant deviation from the ideal bond angle for Co–C1–C2 which was measured at 168.8(3)°. The chloride and alkynyl metal–ligand bond lengths in **Co-L1** are within the range typical for monoalkynyl Co^{III}(cyclam) species of ca. 2.3 and 1.9 Å, respectively. The metal bound C≡C bond length in **Co-L1** (1.208(4) Å) is virtually identical to that of the elongated silyl capped trimer 3,9-bis(triisopropylsilylethynyl)-2,10-dimethyl-6-isopropylidene-2,9-undecadiene-4,7-diyne[18] with a bond length of 1.206(5) Å, and slightly longer than the 1.198(3) Å bond length reported for the analogous complex [Co(cyclam)(*gem*-DEE-H)Cl]$^+$.[47] The only notable deviation in bond lengths in **Co-L1** from the silyl capped trimer structure is the shortening of the free ethynyl C≡C bond length (1.156(5) Å). The bimetallic structure of **Co-L1-Co** is located slightly offset of a crystallographic inversion center, inducing whole molecule disorder for the cation. **Co-L1-Co** has a similar geometry about the Co^{III} center as **Co-L1**. The axial ligands in **Co-L1-Co** are nearly linear with a C1–Co–Cl bond angle of 178.2(5)°. The L1 ligand in **Co-L1-Co** crystallized in the all *s*-trans orientation. The approximately C_2-symmetrical molecule is essentially planar with a maximum deviation from the least-squares plane of the carbon and cobalt framework (excluding the cyclam ring) of 0.0531 Å. The through-space cobalt–cobalt distance within one cation was refined to 11.609(2) Å.

The C_2 symmetric complex {**Co-L2-**}$_2$ crystallized in an all *s*-trans orientations with an inversion center that bisects the C14 enyne bridge. The environment about cobalt in {**Co-L2-**}$_2$ is like **Co-L1**, however with a slightly more linear Cl–Co–C1 bond angle of 178.68(18). The through space Co–Co distance is the longest reported for any dicobalt cyclam complexes at 17.99(3) Å, which is slightly longer than the hexayne complex

DOI: 10.1021/acs.organomet.9b00313
Organometallics 2019, 38, 2758–2769

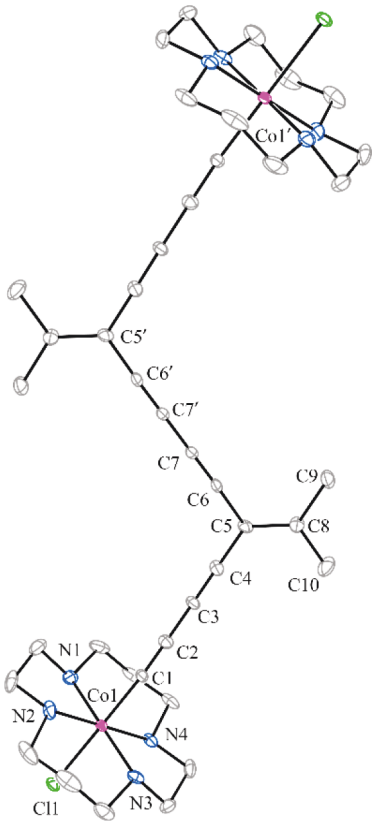

Figure 5. Molecular plot of $[\{\textbf{Co-L2-}\}_2]^{2+}$ at 30% probability level. Hydrogen atoms, solvent molecules, and counterions were omitted for clarity. Inversion symmetry operator for $[\{\textbf{Co-L2-}\}_2]^{2+}$: $-x + 1$, $-y + 2$, $-z + 1$.

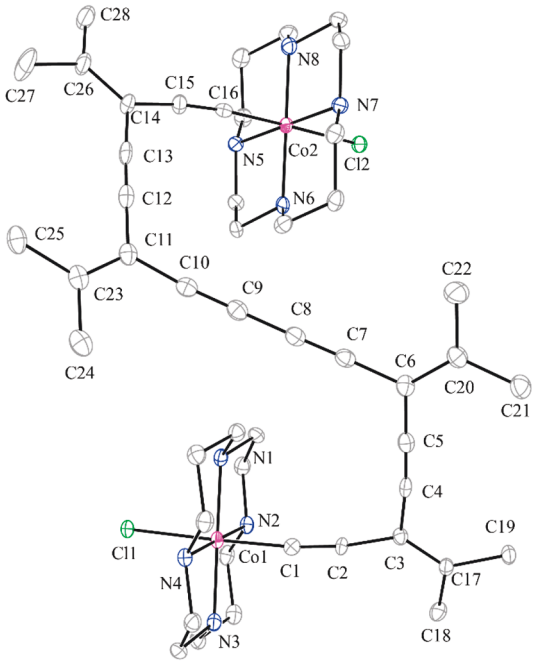

Figure 6. Molecular plot of $[\{\textbf{Co-L1}\}_2]^{2+}$ at 30% probability level. Only one of two symmetry independent cations is shown. Hydrogen atoms, solvent molecules, counterions, and label suffixes were omitted for clarity.

$[\{Co(cyclam)Cl\}_2(\mu\text{-}C_{12})]^{+2}$ reported at 17.6(4) Å.[40] The Co−C1 bond length is 1.873(5) Å, which is within error of the bond distance reported for the oligoynyl complex $[\{Co(cyclam)Cl\}_2(\mu\text{-}C_{12})]^{+2}$ at 1.866(6) Å, but shorter than the tetrayne cross-conjugated complex $[\{Co(cyclam)Cl\}_2(\mu\text{-}gem\text{-}DEE)_2]^{+2}$ at 1.882(2) Å.[47] The decreased cobalt-alkynyl bond leads to an elongated C1≡C2 bond length of 1.218(7) Å. The dimerized **L2** framework has a deviation from the least-squares plane of the carbon and cobalt framework (excluding the cyclam ring) of 0.0504 Å.

Similar crystallization conditions yielded suitable crystals of the dimerized C16 complex $\{\textbf{Co-L1}\}_2$. Surprisingly, the hexayne structure of $\{\textbf{Co-L1}\}_2$ did not adopt an all *s*-trans configuration. Of the 16 possible conformations, $\{\textbf{Co-L1}\}_2$ adopts an *s*-cis conformation like **Co-L1** that is then bridged together in a *s*-trans conformation. This configuration results in a unique twisted conformation that results in a relativity close Co−Co distance of 10.116(1) and 10.070(1) Å (for two crystallographically independent molecules in the structure), which is closer in space than the C8 triyne complex **Co-L1-Co**. Although not as extensive as **Co-L1**, the Co−C1−C2 angles in $\{\textbf{Co-L1}\}_2$ deviate from linearity at 174.3(5)° and 172.8(6)°, respectively. The Co−C1 bond lengths in $\{\textbf{Co-L1}\}_2$ are within error for typical cobalt-alkynyl bonds at 1.867(6) and 1.891(6) Å. All other structural parameters are essentially the same and are comparable to other reported enyne scaffolds.

Intrigued by the unprecedented structural behavior in $\{\textbf{Co-L1}\}_2$, a more detailed investigation of the crystal packing and ligand orientation was performed. The crystal packing in $\{\textbf{Co-L1}\}_2$ revealed a van der Waals interaction between two internal olefins with intermolecular distances of 3.785 and 3.750 Å (Figure S34). Furthermore, an even shorter interaction between C5B and C26A of 3.426 Å was observed. The observed interaction between olefins, enabled by the uncommon *s*-cis conformation, is not present in any of the *s*-trans structures of **Co-L1-Co** or $\{\textbf{Co-L2}\}_2$ (Figure S35). Due to the twisted all *s*-trans configuration cations of $\{\textbf{Co-L1}\}_2$ they are axially chiral, despite of the absence of any chiral centers, and both enantiomers are present in the unit cell of $\{\textbf{Co-L1}\}_2$ related by a crystallographic inversion center. The twisted nature responsible for the axial chirality is caused by a rotation around the axis of the middle bisalkynyl unit of C6 to C11. Both half of the π-frameworks, including the middle bisalkynyl unit either cobalt and chlorine atom 1 or 2, respectively, are virtually planar, with maximum deviations from planarity of 0.2706, 0.1484, 0.4843, and 0.4235 Å from their respective least-squares planes. The twist angles around the C6−C11 bisalkynyl units, based on the above least-squares planes, are 76.031(24) and 78.757(24)° in the two crystallographically independent molecules.

Electrochemistry. Cross-conjugated frameworks often possess electronic properties distinct from their linear structural isomers.[17] With this in mind, it is of interest to probe the electronic properties of the cross-conjugated complexes reported herein. The monoalkynyl complexes **Co-L1** and **Co-L2** possess two redox events within the potential window allowed by MeCN, namely the irreversible reduction of Co^{III} to Co^{II} (**A**) and the reduction of Co^{II} to Co^{I} (**B**) (Scheme 3).[40,44] The first reduction of **Co-L1** occurs at −1.64 V, which is cathodically shifted by 10 mV from that of $[Co(cyclam)(gem\text{-}DEE\text{-}H)Cl]^+$ and does not correlate with the linear triyne analogue $[Co(cyclam)(C_6{-}H)Cl]^+$ (Figure 7).[40,47] In fact, **Co-L1** best matches the potential for

DOI: 10.1021/acs.organomet.9b00313
Organometallics 2019, 38, 2758−2769

Table 1. Selected Bond Lengths (Å) and Bond Angles (deg) for [Co-L1]$^+$, [Co-L1-Co]$^{2+}$, [{Co-L2-}$_2$]$^{2+}$, and [{Co-L1-}$_2$]$^{2+}$

[Co-L1]$^+$		[Co-L1-Co]$^{2+a}$		[{Co-L2-}$_2$]$^{2+}$		[{Co-L1-}$_2$]$^{2+c}$	
Co1−N1	1.962(2)	Co1−N1	1.973(8)	Co1−N1	1.975(4)	Co1−N1	1.974(4)
Co1−N2	1.979(3)	Co1−N2	2.006(9)	Co1−N2	1.962(5)	Co1−N2	1.976(5)
Co1−N3	1.985(3)	Co1−N3	1.993(8)	Co1−N3	1.983(4)	Co1−N3	1.974(4)
Co1−N4	1.978(3)	Co1−N4	2.006(10)	Co1−N4	1.985(5)	Co1−N4	1.974(4)
						Co2−N5	1.973(4)
						Co2−N6	1.972(4)
						Co2−N7	1.973(4)
						Co2−N8	1.975(4)
Co1−C1	1.881(3)	Co1−C1	1.953(9)	Co1−C1	1.873(5)	Co1−C1	1.867(6)
						Co2−C16	1.877(5)
Co1−Cl1	2.3144(8)	Co1−Cl1	2.434(8)	Co1−Cl1	2.3037(14)	Co1−Cl1	2.3191(15)
						Co2−Cl2	2.3155(15)
C1−C2	1.208(4)	C1−C2	1.268(10)	C1−C2	1.218(7)	C1−C2	1.212(7)
C2−C3	1.442(4)	C2−C3	1.504(10)	C2−C3	1.369(7)	C2−C3	1.435(7)
C3−C4	1.431(4)	C3−C4	1.457(11)	C3−C4	1.213(7)	C3−C4	1.442(8)
C4−C5		C4−C4B	1.249(10)	C4−C5	1.425(7)	C4−C5	1.183(8)
C5−C6	1.437(4)			C5−C6	1.451(7)	C5−C6	1.439(8)
C6−C7	1.453(4)			C6−C7	1.193(7)	C6−C7	1.445(8)
C7−C8	1.156(5)			C7−C7′^{b}	1.375(9)	C15−16	1.204(7)
C3−C9	1.359(4)	C3−C5	1.356(10)	C5−C8	1.354(7)	C3−C17	1.348(7)
C6−C12	1.351(4)					C6−C20	1.359(7)
Co1−C1−C2	168.8(3)	Co1−C2−C3	174.4(11)	Co1−C2−C3	175.9(5)	Co1−C1−C2	174.3(5)
						Co2−C16−C15	174.1(5)
Cl1−Co1−C1	176.91(9)	Cl1−Co1−C1	178.2(5)	Cl1−Co1−C1	178.68(18)	Cl1−Co1−C1	178.53(18)
						Cl2−Co2−C16	177.94(17)
		Co1−Co1B	11.609(2)	Co1−Co1′	17.991(3)	Co1A−Co2A	10.116(1)
						Co1B−Co2B	10.070(1)

^{a}Structural disorder of the cation by whole molecule disorder around an inversion center is present. Tabulated values are for one-half molecule. ^{b}Inversion symmetry operator for [{Co-L2-}$_2$]$^{2+}$: $-x + 1, -y + 2, -z + 1$. ^{c}Two symmetry independent cations are present in [{Co-L1-}$_2$]$^{2+}$. Values tabulated are for cation A (label suffixes omitted).

Scheme 3. General Reduction Pathway for Co^{III}(cyclam) Monoalkynyl Complexes

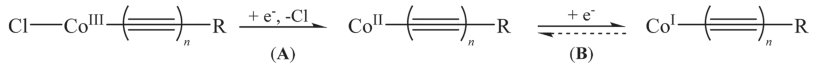

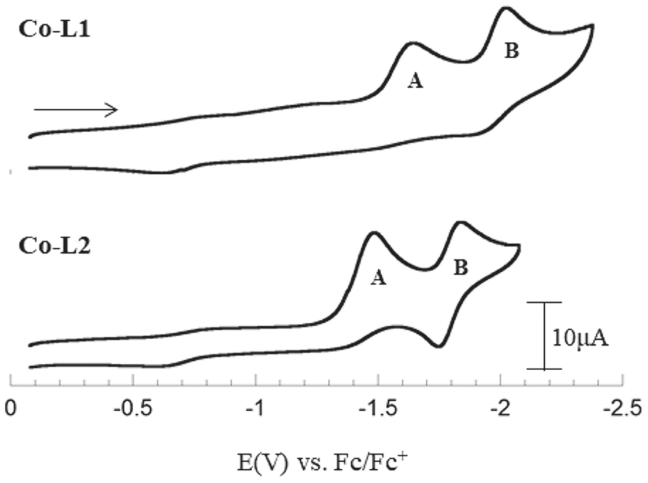

Figure 7. CVs of **Co-L1** (top) and **Co-L2** (bottom) in 0.1 M MeCN solution of Bu_4NBF_4 at a scan rate of 0.10 V/s.

[Co(cyclam)(C$_2$TMS)Cl]$^+$ (−1.60 V).[40] The second reduction of **Co-L1** is essentially irreversible at E_{pc} of −2.02 V with only a slight return of back current. The first reduction of **Co-L2** is anodically shifted by 16 mV from that of **Co-L1** (Table 2). The potential of **Co-L2** is cathodically shifted by approximately 4 mV from the potential of the linear diyne complex [Co(cyclam)(C$_4$−H)Cl]$^+$.[40] The second reduction of **Co-L2** is reversible and tracks closely to the characteristics observed for [Co(cyclam)(C$_4$−H)Cl]$^+$.[40] The trends in electrochemical potential and redox behavior for the monoalkynyl complexes **Co-L1** and **Co-L2** indicate that the electronic properties about Co^{III} best reflect the conjugation prior to the closest intervening olefin.

Table 2. Electrode Potentials (V, vs Fc/Fc$^+$) of Co-L1 and Co-L2

complex	E_{pc} (A) V	E_{pc} (B) V
Co-L1	−1.64	−2.02
Co-L2	−1.48	−1.72 (91, 0.87)
[Co(cyclam)(*gem*-DEE-H)Cl]$^+$ [47]	−1.54	−1.86
[Co(cyclam)(C$_4$H)Cl]$^+$ [40]	−1.42	−1.78

Similar to the monoalkynyl complexes the bimetallic complexes **Co-L1-Co** possess two redox events within the solvent window allowed by MeCN (Figure 8). The electrochemical potentials of the bimetallic compound **Co-L1-Co** is virtually identical to those of **Co-L1** with the only difference being the increase in current owing to the presence of two Co^{III}(cyclam) units (Table 3). The dimeric complex {**Co-L1-**}$_2$ has two irreversible two electron reductions at −1.67 V

DOI: 10.1021/acs.organomet.9b00313
Organometallics 2019, 38, 2758−2769

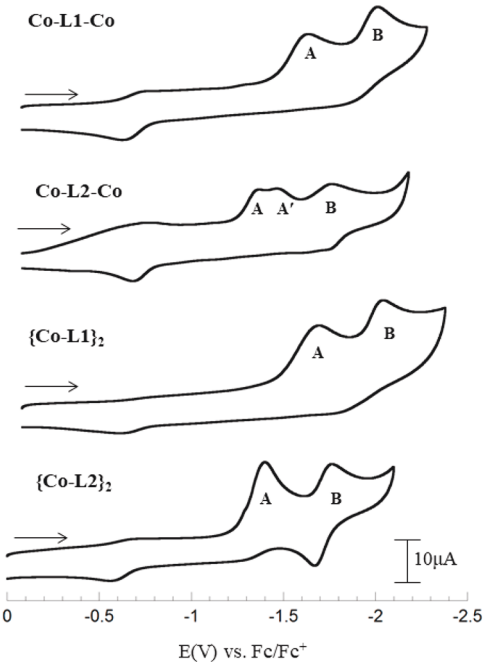

Figure 8. CVs of **Co-L1-Co** (top), **Co-L2-Co** (middle-top), {**Co-L1-**}$_2$ (middle-bottom), and {**Co-L2-**}$_2$ (bottom) in 0.1 M MeCN solution of Bu_4NBF_4 at a scan rate of 0.10 V/s.

Table 3. Electrode Potentials (V, vs Fc/Fc^+) of Co-L1-Co, Co-L2-Co, {Co-L1-}$_2$, and {Co-L2-}$_2$

complex	E_{pc} (A)	E_{pc} (B)
Co-L1-Co	−1.64	−2.01
Co-L2-Co	−1.37 (A), −1.47 (A′)	−1.76
{**Co-L1-**}$_2$	−1.67	−2.04
{**Co-L2-**}$_2$	−1.40 (94, 0.93)	−2.04
[{Co(cyclam) Cl}$_2$ μ-(C_4)]$_2$[40]	−1.44	−1.85
[{Co(cyclam) Cl}$_2$ μ-(*gem*-DEE)]$_2$[44]	−1.58	−1.95
[{Co(cyclam) Cl}$_2$ μ-(*gem*-DEE)$_2$]$_2$[44]	−1.58	−1.87

and −2.04 V. These electrochemical results are intriguing as the addition of a second cobalt unit or oligomerization of the enyne framework does not influence the reduction potentials across the L1 series. In contrast, a gradual anodic shift in Co-based reductions was observed as the oligoyn-diyl elongates in Co—(C≡C)$_n$—Co complexes.[48]

Three redox events are observed in the CV of **Co-L2-Co** and highlight the unsymmetrical alkynyl binding modes at cobalt. Butadiyne is more electron deficient than acetylene, and so it follows that the initial reduction at −1.37 V is likely the single reduction of the butadiynyl-Co(cyclam) unit. This also matches closely with the observed potentials for **Co-L2** and [Co(cyclam)(C_4−H)Cl]$^+$.[40] Thus, the remaining single electron reduction at −1.47 is the reduction of the second cobalt unit bound to the ethynyl moiety. An irreversible two electron reduction of both cobalt species to Co^I is observed at −1.76. The symmetrical dimeric complex {**Co-L2-**}$_2$ has a single two electron reduction at −1.40 V. A reversible two electron reduction to the Co^I species in {**Co-L2-**}$_2$ is measured at −2.04 V.

Our results clearly show that electronic interaction between Co(cyclam) units diminishes upon the addition of intervening olefins, and the reported bimetallic complexes are best described as covalently linked but electronically isolated Co^{III} species. Electronic isolation of the Co^{III} centers is further supported by DPV analysis for the reported dicobalt complexes which all have ΔE_p values consistent with valence isolated systems (Figure S16−S21).

DFT Calculations. To evaluate both electronic structures and orbital interactions across the reported enyne frameworks, spin-restricted density functional calculations were performed on the geometrically optimized model cations [**Co-L1-Co**]$^{2+}$, [**Co-L2-Co**]$^{2+}$, [{**Co-L1-**}$_2$]$^{2+}$, [{**Co-L2-**}$_2$]$^{2+}$, and [{Co-(cyclam)Cl}$_2$(μ-*gem*-DEE)$_2$](PF_6)$_2$[44] [{**Co-DEE-**}$_2$]$^{2+}$ at the B3LYP/LanL2DZ level using the Gaussian 16 suite.[49] Optimized bond lengths are reported in Table 4 with structural models presented in the Supporting Information. The coordination environment about cobalt is nearly identical in bond angles and bond lengths to the data from crystallographic

Table 4. Select DFT-Optimized Bond Lengths (Å) and Angles for Complexes [Co-L2-Co]$^{2+}$, [Co-L1-Co]$^{2+}$, [{Co-DEE-}$_2$]$^{2+}$,[{Co-L2-}$_2$]$^{2+}$, and [{Co-L1-}$_2$]$^{2+}$

[**Co-L2-Co**]$^{2+}$		[**Co-L1-Co**]$^{2+}$		[{**Co-DEE-**}$_2$]$^{2+}$		[{**Co-L2-**}$_2$]$^{2+}$		[{**Co-L1-**}$_2$]$^{2+}$	
Co−N_{avg}	2.012	Co−N_{avg}	2.012	Co−N_{avg}	2.012	Co−N_{avg}	2.012	Co−N_{avg}	2.012
Co1−C1	1.911	Co1−C1	1.914	Co1−C1	1.910	Co1−C1	1.904	Co1−C1	1.901
Co2−C	1.913	Co2−C8	1.914	Co2−C10	1.910	Co2−C14	1.904	Co2−C16	1.908
Co1−Cl1	2.370	Co1−Cl1	2.377	Co1−Cl1	2.378	Co1−Cl1	2.374	Co1−Cl1	2.385
Co2−Cl2	2.376	Co2−Cl2	2.377	Co2−Cl2	2.378	Co2−Cl2	2.375	Co2−Cl2	2.381
C1−C2	1.245	C1−C2	1.240	C1−C2	1.239	C1−C2	1.244	C1−C2	1.238
C2−C3	1.376	C2−C3	1.450	C2−C3	1.450	C2−C3	1.375	C2−C3	1.449
C3−C4	1.233	C3−C4	1.442	C3−C4	1.438	C3−C4	1.232	C3−C4	1.442
C4−C5	1.440	C4−C5	1.229	C4−C5	1.234	C4−C5	1.439	C4−C5	1.229
C5−C6	1.449					C5−C6	1.436	C5−C6	1.441
C6−C7	1.240					C6−C7	1.233	C6−C7	1.437
						C7−C8	1.369	C7−C8	1.234
								C8−C9	1.370
C5−C8	1.381	C3−C9	1.379	C3−C11	1.380	C5−C15	1.382	C3−C17	1.376
								C6−C20	1.382
Co1−C1−C2	177.5	Co1−C2−C3	179.0	Co1−C2−C3	178.0	Co1−C1−C2	176.5	Co1−C2−C3	176.4
Cl1−Co1−C1	178.7	Cl1−Co1−C1	176.2	Cl1−Co1−C1	178.4	Cl1−Co1−C1	178.8	Cl1−Co1−C1	177.6
Co1−Co2	10.478	Co1−Co2	11.578	Co1−Co2	13.388	Co1−Co2	18.272	Co1−Co2	16.404

DOI: 10.1021/acs.organomet.9b00313
Organometallics 2019, 38, 2758−2769

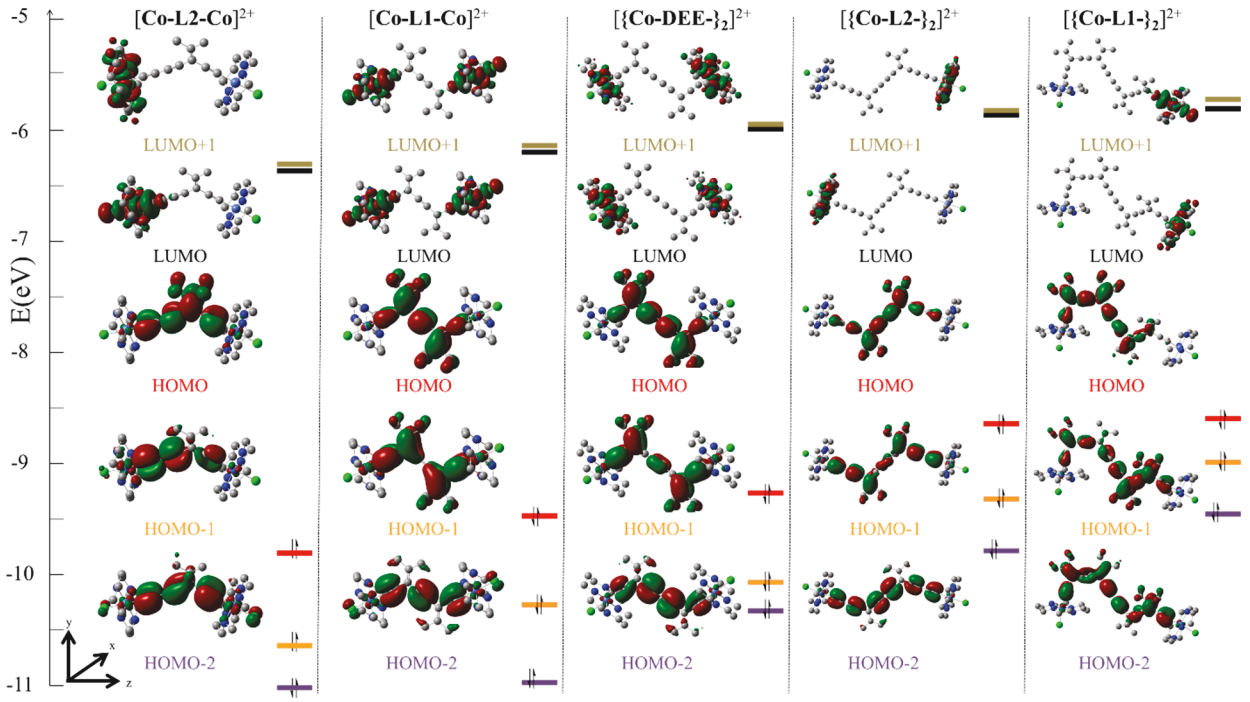

Figure 9. Molecular orbital diagram for the frontier orbitals of compound [**Co-L2-Co**]$^{2+}$, [**Co-L1-Co**]$^{2+}$, [{**Co-DEE-**}$_2$]$^{2+}$, [{**Co-L2-**}$_2$]$^{2+}$, and [{**Co-L1-**}$_2$]$^{2+}$ obtained from DFT calculation.

analysis. Only a slight elongation of the Co−C bonds (ca. 0.05 Å) is observed across the series, but still within the expected distances for the covalent radius of a cobalt and a carbon atom, also leading to a slight elongation of the metal bound C≡C bond. This behavior is typical for transition metal alkynyl complexes.[50] Furthermore, the general trend of decreased C1−C2 bond length as the bridge length increases is also observed in the optimized structures of [**Co-L2-Co**]$^{2+}$, [**Co-L1-Co**]$^{2+}$, [{**Co-DEE-**}$_2$]$^{2+}$, and [{**Co-L1-**}$_2$]$^{2+}$. The lowest energy orientation of the enyne framework for [**Co-L1-Co**]$^{2+}$, [{**Co-L2-**}$_2$]$^{2+}$, and [{**Co-DEE-**}$_2$]$^{2+}$ was found to be the all *s*-trans configuration (Figure S36−S39). Notably the orientation for [{**Co-L1-**}$_2$]$^{2+}$ did not follow this trend (Figure S40). Nor did the computational orientation of [{**Co-L1-**}$_2$]$^{2+}$ match the orientation observed in the crystallographic structure (*s*-cis−trans−cis). In fact, the lowest energy conformation was found to be an *s*-trans−trans−cis configuration. Along the optimization pathway the all *s*-trans configuration was higher by only 0.054 V and the crystallographic configuration at 0.017 V, indicating that in solution potentially all 16 geometric polymorphs are possible. The through space bond distances between cobalt centers matches closely with crystallographic analysis, with the only exception being [{**Co-L1-**}$_2$]$^{2+}$ which is elongated by ca. 6 Å in the computational optimization structure.

Frontier molecular orbitals of acyclic cross conjugated systems were reported by Luthi and co-workers using both density functional theory (DFT) and ab initio methods.[51,52] Our laboratory has also been interested in calculating metal−metal interactions across nonlinear enyne bridges based on DFT calculations of hypothetical [M]-*gem*-DEE-[M] with [M] representing 3*d* metal complexes of dppe.[44,53] To expand these studies to bridge lengths beyond five carbons, frontier molecular orbitals were calculated for the complexes reported herein. The computed contour plots and energy levels for the frontier molecular orbitals are shown in Figure 9. A general increase in energy is observed as bridge length increases across the series which is similar to what was reported for oligoyndiyl bridge complexes.[40] The E_g values for the L1 series is less perturbed by bridge length than the L2 series and far less than the oligoyndiyl series, which is reflected in the cyclic voltammetry ($E_{p,c}$(A)).[40] Complexes [**Co-L2-Co**]$^{2+}$, [**Co-L1-Co**]$^{2+}$, [{**Co-DEE-**}$_2$]$^{2+}$, and [{**Co-L2-**}$_2$]$^{2+}$ have similar HOMO, HOMO−1, and HOMO−2 contour plots, which represent part of the filled Co t_{2g} set. It is clear from Figure 9 that the HOMO and HOMO−1 is a combination of the d_{xz}(Co) with the antibonding combination of the $\pi_\perp$(enyne) (perpendicular, out-of-plane (C≡C)) orbitals and vinyl π(C═C). The HOMO−2 is composed of the antibonding combination of the d_{yz} (Co) and the antibonding $\pi_\parallel$(DEE) (parallel, in-plane (C≡C)) orbitals, without contribution from the vinyl π(C═C) unit. Compounds [{**Co-L1-**}$_2$]$^{2+}$ is nearly void of any cobalt-bridge interaction.

The LUMO and LUMO+1 in [{**Co-DEE-**}$_2$]$^{2+}$, [{**Co-L1-**}$_2$]$^{2+}$, [{**Co-L2-**}$_2$]$^{2+}$ are dominated by the antibonding combination of the $d_{x^2-y^2}$ (Co) with the *p*-orbitals of the surrounding cyclam N atoms, with no contribution from either of the axial ligands. This is in contrast with the orbital assembly in complexes [**Co-L1-Co**]$^{2+}$, [**Co-L2-Co**]$^{2+}$, where the LUMOs have some mixing of the d_{z^2} (Co) with the σ* based orbitals on the enyne bridge. Orbital mixing in the LUMOs spanning the entirety of the cross-conjugated bridge is not observed for the reported enyne complexes. This was not the case for shorter cobalt-*gem*-DEE complexes, which showed, albeit weak, orbital interactions that spanned the entirety of the bridge.[44] These results are not atypical, as it is well-known that increased bridge length leads to weaker metal−metal interaction. Furthermore, this result and others suggest that increased substitution of the intervening olefin leads to successively less metal−metal interaction.[41]

DOI: 10.1021/acs.organomet.9b00313
Organometallics 2019, 38, 2758−2769

CONCLUSION

A series of monomeric, bimetallic, and dimeric Co^{III} cyclam complexes bearing extended acyclic enyne frameworks of L1 or L2 were prepared in modest to good yields. Complexes reported herein, including the dimeric C14 and C16 bridged complexes, were stable for structural and electronic characterization. Crystallographic analysis of dimeric complexes, {**Co-L1-**}$_2$ and {**Co-L2-**}$_2$, revealed a pseudo-octahedral geometry about both Co^{III} units that are bridged in the apical direction by the unsaturated enyne scaffolds. The C14 bridged complex {**Co-L2-**}$_2$ has the longest crystallographic through-space Co−Co distance of 17.991(3) Å. The C16 bridged complex {**Co-L1-**}$_2$ exhibits an unprecedented *s*-cis−trans−cis orientation leading to a twisted axially chiral configuration of the cations that pack in the solid state as pairs of enantiomers and packing is stabilized by close intermolecular $\pi-\pi$ interactions. Cyclic voltammetry measurements show valence isolation with redox potentials modulated by the first intervening olefin. DFT analysis calculated substantial mixing of orbitals in the HOMOs of the dinuclear cobalt-L1 and -L2 complexes, with weak and incomplete mixing of orbitals across the LUMOs. Isolation and characterization of the extended transition-metal enyne complexes reported herein illustrate the rich structural diversity and electronic properties within this family of enyne compounds.

EXPERIMENTAL SECTION

General Procedures. All reagents were used as received. Starting materials [Co(cyclam)Cl_2]Cl,[54] L1,[18] and L2[39] were prepared according to literature procedures. Tetrahydrofuran was freshly distilled over sodium/benzophenone. UV−vis spectra were obtained with a Jasco V-670 spectrophotometer. FT-IR spectra were measured on a Jasco FT/IR-6300 as neat samples. ^{1}H NMR spectra were obtained using a Varian Mercury 300 NMR, with chemical shifts (δ) referenced to the residual solvent signal (CH_3CN). Elemental analysis (EA) was performed by Atlantic Microlab, Norcross, GA. Electrospray ionization mass spectrometry (ESI-MS) spectra were recorded by direct injection onto a Waters 600 LC−MS. Voltammograms were recorded on a CHI620A voltammetric analyzer with a glassy carbon working electrode (diameter = 2 mm), a Pt-wire auxiliary electrode, and a $Ag/AgNO_3$ reference electrode filled with 10 mM $AgNO_3$ and 0.1 M Bu_4NBF_4 in dry MeCN. The concentration of analyte is always 1.0 mM in 4 mL dry MeCN (thoroughly degassed by Ar purging). Potentials were corrected using an internal ferrocene standard at the end of runs.

*Preparation of [Co(cyclam)(L1)Cl]Cl (**Co-L1**).* In a round-bottom flask 500 mg (1.37 mmol) of [Co(cyclam)Cl_2]Cl was dissolved in 250 mL of MeOH. To the solution was added 1.0 mL (7.2 mmol) of Et_3N and 300 mg (1.65 mmol) of L1. The solution was refluxed for 16 h, and a gradual shift in solution color from green to red was observed. Solvent was removed in vacuo, and purification was performed on a silica gel pad by rinsing with EtOAc, and then eluting [Co(cyclam)-(L1)Cl]Cl with a EtOAc/MeOH (5:1) mixture. The chloride salt can be isolated in high purity;[40,44] however, due to limited solubility of elongated frameworks in organic solution, the counterion was exchanged as follows. Solvent was removed, and [Co(cyclam)(L1)-Cl]Cl was dissolved in 50 mL MeOH. A concentrated solution of $NaPF_6$ (0.100 g, 6.92 mmol) in MeOH was added, causing a light orange solid to precipitate. The solid was filtered off, transferred to a small silica pad with DCM and eluted with 1:2 MeCN:DCM. Solvent was removed and the residue recrystallized by addition of Et_2O to a concentrated solution in MeCN to give orange needle crystals of **Co-L1**. Yield: 644 mg (1.03 mmol) (76% based on Co). Data for **Co-L1**: ESI-MS (MeOH): 475.5-[Co(cyclam)(L1)Cl]$^+$. Elem. Anal. Found (calcd) for $C_{24}H_{41}N_4ClO_2Co\cdot PF_6$ (**Co-L1**·$2H_2O$) C, 44.12 (43.88); H, 6.34 (6.29); N, 8.39 (8.53). IR (cm^{-1}) —C≡C—H 2106 (s), (Co—C≡C—) 2099 (s). ^{1}H NMR (CD_3CN, δ) 4.379 (br s, 2H, N-*H*), 4.236 (br s, 2H, N-*H*), 3.288 (s, 1H, C≡C*H*), 2.775−2.305 (m, 16H, CH_2), 2.042 (s, 6H, CH_3), 1.940 (s, 6H, CH_3), 1.866 (t, 2H, CH_2, J = 14.4 Hz), 1.349 (q, 2H, CH_2). Absorption spectrum (MeCN) λ_{max} nm (ε_{max}, M^{-1} cm^{-1}) 490 (160), 302 (11 963).

*Preparation of [Co(cyclam)(L2)Cl]PF_6 (**Co-L2**).* In a round-bottom flask 500 mg (1.37 mmol) of [Co(cyclam)Cl_2]Cl was dissolved in 250 mL of MeOH. To the solution was added 1.0 mL (7.2 mmol) of Et_3N and 210 mg (1.64 mmol) of L2. The solution was refluxed for 40h, and a gradual shift in solution color from green to red was observed. Solvent was removed in vacuo, and purification was performed on a silica gel pad by rinsing with EtOAc, and then eluting [Co(cyclam)-(L2)Cl]Cl with a EtOAc/MeOH (5:1) mixture. The chloride salt can be isolated in high purity;[40,44] however, due to limited solubility of elongated frameworks in organic solution, the counterion was exchanged as follows. Solvent was removed in vacuo, and [Co-(cyclam)(L2)Cl]Cl was dissolved in 50 mL MeOH. A concentrated solution of $NaPF_6$ (0.100 g, 6.92 mmol) in MeOH was added, causing a light orange solid to precipitate. The solid was filtered off, transferred to a small silica pad with DCM and eluted with 1:2 MeCN:DCM. Solvent was removed in vacuo and the residue recrystallized by addition of Et_2O to a concentrated solution in MeCN to give an orange powder of **Co-L2**. Yield: 318 mg (0.56 mmol) (41% based on Co). Data for **Co-L2**: ESI-MS (MeCN) 421.4-[Co(cyclam)(L2)Cl]$^+$. Elem. Anal. Found (calcd) for $C_{20}H_{37}N_4ClO_3Co\cdot PF_6$ (**Co-L2**·$3H_2O$) C, 39.04 (38.69); H, 6.24 (6.01); N, 9.17 (9.02). IR (cm^{-1}) —C≡C—H 2187 (s), (Co—C≡C—) 2063 (s). ^{1}H NMR (CD_3CN, δ) 4.382 (br s, 4H, N-*H*), 3.268 (s, 1H, C≡C*H*), 2.675−2.251 (m, 16H, CH_2), 2.022 (s, 3H, CH_3), 1.946 (s, 3H, CH_3), 1.810 (t, 2H, CH_2, J = 14.4 Hz), 1.329 (q, 2H, CH_2). Absorption spectrum (MeCN) λ_{max} nm (ε_{max}, M^{-1} cm^{-1}) 490 (193), 303 (14 915), 286 (17 949), 272 (14 142).

*Preparation of [{Co(cyclam)Cl}$_2$(μ-L1)](PF$_6$)$_2$(**Co-L1-Co**).* Method A: In a round-bottom flask 100 mg (0.20 mmol) of [Co(cyclam)-(L1)Cl]Cl was dissolved in 100 mL of MeOH. To the solution was added 0.5 mL (3.6 mmol) of Et_3N and 86 mg (0.23 mmol) of [Co(cyclam)Cl_2]Cl. The solution was refluxed for 16h, and a gradual shift in solution color from olive green to orange-red was observed. Solvent was removed in vacuo, and purification was performed on a silica gel pad by rinsing with EtOAc, and then eluting [{Co(cyclam)-Cl}$_2$(μ-L1)](Cl)$_2$ with a gradual increased gradient of an EtOAc/MeOH (up to 1:1) mixture. Solvent was removed in vacuo, and [{Co(cyclam)Cl}$_2$(μ-L1)](Cl)$_2$ was dissolved in 50 mL MeOH. A concentrated solution of $NaPF_6$ (0.100 g, 6.92 mmol) in MeOH was added, causing a light orange solid to precipitate. The solid was filtered off, transferred to a small silica pad with DCM and eluted with 1:2 MeCN:DCM. Solvent was removed in vacuo and the residue recrystallized by addition of Et_2O to a concentrated solution in MeCN to give red needle crystals of **Co-L1-Co**. Yield: 162 mg (0.15 mmol) (78% based on Co). Data for **Co-L1-Co**: ESI-MS (MeCN) 385.2-[{Co(cyclamCl}$_2$(μ-*gem*-DEE)]$^{2+}$, 913.5-[{{Co(cyclam)-Cl}$_2$(μ-L1)}}PF_6]$^+$. Elem. Anal. Found (calcd) for $C_{35}H_{64}N_8Cl_2OCo_2\cdot(PF_6)_2$ (**Co-L1-Co**·CH_3OH) C, 38.25 (38.51); H, 5.80 (5.91); N, 10.09 (10.26). IR (cm^{-1}) —C≡C— 2178 (s), (Co—C≡C—) 2110 (s). ^{1}H NMR (CD_3CN, δ) 4.397 (br s, 4H, N-*H*), 4.215 (br s, 4H, N-*H*), 2.675−2.251 (m, 32H, CH_2), 2.071 (s, 6H, CH_3), 1.870 (s, 6H, CH_3), 1.736 (t, 4H, CH_2, J = 14.4 Hz), 1.388 (q, 4H, CH_2). Absorption spectrum (MeCN) λ_{max} nm (ε_{max}, M^{-1} cm^{-1}) 481 (353), 304 (17 531), 285 (22 662).

Method B: In a round-bottom flask 250 mg (0.68 mmol) of [Co(cyclam)Cl_2]Cl was dissolved in 150 mL of MeOH. To the solution was added 0.5 mL (3.6 mmol) of Et_3N and 57 mg (0.31 mmol) of L1. The solution was refluxed for 16h, and a gradual shift in solution color from green to red was observed. Solvent was removed in vacuo, and purification was performed on a silica gel pad by rinsing with EtOAc, and then eluting [{Co(cyclam)Cl}$_2$(μ-L1)](Cl)$_2$ with a gradual increased gradient of an EtOAc/MeOH (up to 1:1) mixture. Solvent was removed in vacuo, and [{Co(cyclam)Cl}$_2$(μ-L1)](Cl)$_2$ was dissolved in 50 mL MeOH. A concentrated solution of $NaPF_6$ (0.100 g, 6.92 mmol) in MeOH was added, causing a light orange

DOI: 10.1021/acs.organomet.9b00313
Organometallics 2019, 38, 2758−2769

solid to precipitate. The solid was filtered off, transferred to a small silica pad with DCM and eluted with 1:2 MeCN:DCM. Solvent was removed in vacuo and the residue recrystallized by addition of Et_2O to a concentrated solution in MeCN to give a red crystalline material of **Co-L1-Co**. Yield: 406 mg (0.383 mmol) (56% based on Co).

*Preparation of [{Co(cyclam)Cl}$_2$(μ-L2)](PF$_6$)$_2$(**Co-L2-Co**).* Method A: Following an analogous procedure to Method A for the synthesis of **Co-L1-Co** using L2 instead of L1yields **Co-L2-Co**, except in this case an orange powdery material is obtained. Yield: 113 mg (0.11 mmol) (64% based on Co). Data for **Co-L2-Co**: ESI-MS (MeCN) 358.2-[{Co(cyclam)Cl}$_2$(μ-L2)]$^{2+}$, 859.4-[{{Co(cyclam)Cl}$_2$(μ-L2)}}PF$_6$]$^+$. Elem. Anal. Found (calcd) for $C_{30}H_{54}N_8Cl_2Co_2\cdot(PF_6)_2$ (**Co-L2-Co**) C, 35.65 (35.84); H, 5.42 (5.41); N, 10.96 (11.14). IR (cm^{-1}) —C≡C— 2191 (s), (Co—C≡C—) 2112 (s), (Co—C≡C—) 2066 (s). ^{1}H NMR (CD_3CN, δ) 4.492 (br s, 8H, N-*H*), 2.874–2.385 (m, 32H, C*H*$_2$), 2.141 (s, 3H, C*H*$_3$), 1.955 (s, 3H, C*H*$_3$), 1.889 (t, 4H, CH$_2$, *J* = 14.4 Hz), 1.453 (q, 4H, CH$_2$). Absorption spectrum (MeCN) λ_{max} nm (ε_{max}, M^{-1} cm^{-1}) 488 (434), 303 (14 915), 286 (17 949), 272 (14 142).

Method B: An analogous procedure to Method B for the synthesis of **Co-L1-Co** using L2 instead of L1 yields **Co-L2-Co**. Yield: 413 mg (0.41 mmol) (60% based on Co).

*Preparation of [{Co(cyclam)Cl}$_2$(μ-L1)$_2$](PF$_6$)$_2$({**Co-L1-**}$_2$).* In a round-bottom flask 150 mg (0.24 mmol) of **Co-L1** was dissolved in 50 mL of methanol which is sparged with O_2. To the solution was added Hay catalyst (0.05 g CuCl (0.5 mmol), 0.20 mL (1.3 mmol) TMEDA in 3 mL of MeOH) and the solution was purged with O_2 for 6h. Solvent was removed in vacuo and the residue was transferred to a small silica pad with DCM and eluted with a MeCN/DCM (1:2) mixture. Compound {**Co-L1-**}$_2$ was then recrystallized by the addition of Et_2O to a concentrated solution in MeCN yielding {**Co-L1-**}$_2$ as an orange crystalline material. Yield: 72 mg (0.06 mmol) (24% based on **Co-L1**). Data for {**Co-L1-**}$_2$: ESI-MS (MeCN) 475.4-[{Co(cyclam)Cl}$_2$(μ-L1)$_2$]$^{2+}$, 1093.7-[{{Co(cyclam)-Cl}$_2$(μ-L1)$_2$}PF$_6$]$^+$. Elem. Anal. Found (calcd) for $C_{48}H_{76}N_8O_2Co_2Cl_2\cdot 2PF_6$ ({**Co-L1-**}$_2\cdot$2H$_2$O) C, 45.15 (45.19); H, 6.12 (6.00); N, 8.67 (8.78). IR (cm^{-1}) —C≡C— 2262 (s), (—C≡C—) 2188 (s), (Co—C≡C—) 2107 (s). ^{1}H NMR (CD_3CN, δ) 4.47 (br s, 4H, N-*H*), 4.33 (br s, 4H, N-*H*), 2.86–2.40 (m, 32 H, C*H*$_2$), 2.146 (s, 6H, C*H*$_3$), 2.05 (s, 6H, C*H*$_3$), 2.03 (s, 6H, C*H*$_3$), 1.95 (s, 6H, C*H*$_3$), 1.87 (t, 4H, CH$_2$, *J* = 14.7 Hz), 1.44 (q, 4H, CH$_2$). Absorption spectrum (MeCN) λ_{max} nm (ε_{max}, M^{-1} cm^{-1}) 489 (313), 329 (8613), 297 (36 626).

*Preparation of [{Co(cyclam)Cl$_2$}(μ-L2)$_2$)](PF$_6$)$_2$({**Co-L2-**}$_2$).* An analogous procedure for the synthesis of {**Co-L1-**}$_2$ using **Co-L2** instead of **Co-L1** yields {**Co-L2-**}$_2$ as an orange powder. Yield: 99 mg (0.09 mmol) (33% based on **Co-L2**). Data for {**Co-L2-**}$_2$: ESI-MS (MeCN) 420.4-[{Co(cyclam)Cl}$_2$(μ-L2)$_2$]$^{2+}$, 985.4-[{{Co(cyclam)-Cl}$_2$(μ-L2)$_2$}PF$_6$]$^+$. Elem. Anal. Found (calcd) for $C_{40}H_{64}N_8Co_2Cl_2O_2\cdot 2PF_6$ ({**Co-L2-**}$_2\cdot$2H$_2$O) C, 41.43 (41.14); H, 5.32 (5.52); N, 9.74 (9.60). IR (cm^{-1}) (—C≡C—) 2191, (—C≡C—) 2132, (Co—C≡C—) 2064. ^{1}H NMR (CD_3OD, δ) 4.63 (br s, 8H, N-*H*), 2.94–2.54 (m, 32 H, C*H*$_2$), 2.27 (s, 6H, C*H*$_3$), 2.05 (s, 6H, C*H*$_3$), 1.84 (t, 4H, CH$_2$, *J* = 14.7 Hz), 1.51 (q, 4H, CH$_2$). Absorption spectrum (MeCN) λ_{max} nm (ε_{max}, M^{-1} cm^{-1}) 486 (333), 331 (10 574), 311 (18 190), 295 (20 670), 280 (18 428).

X-ray Data Collection, Processing, and Structure Analysis and Refinement for Crystals. X-ray diffraction data were collected on either a Rigaku RAPID-II image plate diffractometer using Cu Kα (λ = 1.54184 Å) radiation, for **Co-L1**, **Co-L1-Co** and {**Co-L1-**}$_2$, or on a Bruker Quest diffractometer using Mo Kα (λ = 0.71073 Å) radiation, for {**Co-L2-**}$_2$. The structures were solved using the structure solution program DIRDIF2008[55] and refined using the SHELXTL suite of programs.[56] Additional data collection and refinement details, including description of disorder (where present) for compounds **Co-L1**, **Co-L1-Co**, {**Co-L1-**}$_2$, and {**Co-L2-**}$_2$ are given in the Supporting Information. Complete crystallographic data, in CIF format, have been deposited with the Cambridge Crystallographic Data Center: CCDC 1845528 (**Co-L1**), 1845529 (**Co-L1-Co**), 1845531 ({**Co-L1-**}$_2$), and 1845530 ({**Co-L2-**}$_2$). These data can be obtained free of charge from The Cambridge Crystallographic Data Centre via www.ccdc.cam.ac.uk/datarequest/cif.

Computational Details. The geometries of [**Co-L2-Co**]$^{2+}$, [**Co-L1-Co**]$^{2+}$, [{**Co-DEE-**}$_2$]$^{2+}$, [{**Co-L2-**}$_2$]$^{2+}$, and [{**Co-L1-**}$_2$]$^{2+}$ in the ground state were fully optimized from the crystal structures, using the density functional method B3LYP (Beck's three-parameter hybrid functional using the Lee–Yang–Parr correlation function) and employing the LanL2DZ basis set. The calculation was accomplished by using the Gaussian16 program package.[49]

■ ASSOCIATED CONTENT

Supporting Information

The Supporting Information is available free of charge on the ACS Publications website at DOI: 10.1021/acs.organomet.9b00313.

Computed Cartesian coordinates of all molecules reported in this study (the file may be opened as a text file to read the coordinates, or opened directly by a molecular modeling program such as Mercury version 3.3 or later, http://www.ccdc.cam.ac.uk/pages/Home.aspx, for visualization and analysis) (XYZ)

IR spectra for all complexes presented, scan rate experiments, differential pulse voltammograms for **Co-L1**, **Co-L2**, **Co-L1-Co**, **Co-L2-Co**, {**Co-L1-**}$_2$, and {**Co-L2-**}$_2$, computational details and relevant geometric parameters for the optimized structures of **Co-L1-Co**, **Co-L2-Co**, {**Co-L1-**}$_2$, {**Co-DEE-**}$_2$, and {**Co-L2-**}$_2$ (PDF)

Accession Codes

CCDC 1845528–1845531 contain the supplementary crystallographic data for this paper. These data can be obtained free of charge via www.ccdc.cam.ac.uk/data_request/cif, or by emailing data_request@ccdc.cam.ac.uk, or by contacting The Cambridge Crystallographic Data Centre, 12 Union Road, Cambridge CB2 1EZ, UK; fax: +44 1223 336033.

■ AUTHOR INFORMATION

Corresponding Authors

*E-mail: natolisn@berkeley.edu.

*E-mail: tren@purdue.edu.

ORCID

Sean N. Natoli: 0000-0003-2966-3820

Matthias Zeller: 0000-0002-3305-852X

Tong Ren: 0000-0002-1148-0746

Notes

The authors declare no competing financial interest.

■ ACKNOWLEDGMENTS

We gratefully acknowledge financial support from the National Science Foundation (CHE 1362214 and CHE 1764347 for research, and CHE 1625543 for X-ray diffractometers). S.N.N. thanks the California Alliance (HRD-1647273) and the Burroughs Wellcome Fund (PDEP) for support during the writing of this manuscript. We wish to dedicate this contribution to Jean-Francois Halet, a dear friend and Maître on electronic structures of carbon rich organometallics, on the occasion of his 60th birthday.

■ REFERENCES

(1) Diederich, F.; Tykwinski, R. R.; Stang, P. J. *Acetylene Chemistry: Chemistry, Biology and Materials Science*; Wiley-VCH: Weinheim, 2004.

DOI: 10.1021/acs.organomet.9b00313
Organometallics 2019, 38, 2758–2769

(2) Ho, C. L.; Wong, W. Y. Charge and energy transfers in functional metallophosphors and metallopolyynes. *Coord. Chem. Rev.* **2013**, *257*, 1614−1649.
(3) Haque, A.; Al-Balushi, R. A.; Al-Busaidi, I. J.; Khan, M. S.; Raithby, P. R. Rise of Conjugated Poly-ynes and Poly(Metalla-ynes): From Design Through Synthesis to Structure-Property Relationships and Applications. *Chem. Rev.* **2018**, *118*, 8474−8597.
(4) Herndon, J. W. The chemistry of the carbon-transition metal double and triple bond: Annual survey covering the year 2017. *Coord. Chem. Rev.* **2018**, *377*, 86−190.
(5) Xu, L.; Ho, C.-L.; Liu, L.; Wong, W.-Y. Molecular/polymeric metallaynes and related molecules: Solar cell materials and devices. *Coord. Chem. Rev.* **2018**, *373*, 233−257.
(6) Ho, C.-L.; Yu, Z.-Q.; Wong, W.-Y. Multifunctional polymetallaynes: properties, functions and applications. *Chem. Soc. Rev.* **2016**, *45*, 5264−5295.
(7) Paul, F.; Lapinte, C. Organometallic Molecular Wires and Other Nanoscale-sized Devices. An Approach using the Organoiron (dppe)Cp*Fe Building Block. *Coord. Chem. Rev.* **1998**, *178−180*, 431−509.
(8) Bruce, M. I.; Low, P. J. Transition Metal Complexes Containing All-Carbon Ligands. *Adv. Organomet. Chem.* **2004**, *50*, 179−444.
(9) Szafert, S.; Gladysz, J. A. Update 1 of: Carbon in One Dimension: Structural Analysis of the Higher Conjugated Polyynes. *Chem. Rev.* **2006**, *106*, 1−33.
(10) Costuas, K.; Rigaut, S. Polynuclear carbon-rich organometallic complexes: clarification of the role of the bridging ligand in the redox properties. *Dalton Trans.* **2011**, *40*, 5643−5658.
(11) Mahapatro, A. K.; Ying, J.; Ren, T.; Janes, D. B. Electronic Transport through Ruthenium Based Redox-Active Molecules in Metal-Molecule-Metal Nanogap Junctions. *Nano Lett.* **2008**, *8*, 2131−2136.
(12) Meng, F. B.; Hervault, Y. M.; Shao, Q.; Hu, B. H.; Norel, L.; Rigaut, S.; Chen, X. D. Orthogonally modulated molecular transport junctions for resettable electronic logic gates. *Nature Commun.* **2014**, No. 3023.
(13) Zhu, H.; Pookpanratana, S. J.; Bonevich, J. E.; Natoli, S. N.; Hacker, C. A.; Ren, T.; Suehle, J. S.; Richter, C. A.; Li, Q. Redox-Active Molecular Nanowire Flash Memory for High-Endurance and High-Density Non-Volatile Memory Applications. *ACS Appl. Mater. Interfaces* **2015**, *7*, 27306−27313.
(14) Solomon, G. C.; Andrews, D. Q.; Goldsmith, R. H.; Hansen, T.; Wasielewski, M. R.; Van Duyne, R. P.; Ratner, M. A. Quantum Interference in Acyclic Systems: Conductance of Cross-Conjugated Molecules. *J. Am. Chem. Soc.* **2008**, *130*, 17301−17308.
(15) Solomon, G. C.; Andrews, D. Q.; Van Duyne, R. P.; Ratner, M. A. When things are not as they seem: Quantum interference turns molecular electron transfer "Rules" upside down. *J. Am. Chem. Soc.* **2008**, *130*, 7788−7789.
(16) Nielsen, M. B.; Diederich, F. Conjugated oligoenynes based on the diethynylethene unit. *Chem. Rev.* **2005**, *105*, 1837−1867.
(17) Gholami, M.; Tykwinski, R. R. Oligomeric and polymeric systems with a cross-conjugated pi-framework. *Chem. Rev.* **2006**, *106*, 4997−5027.
(18) Zhao, Y.; Tykwinski, R. R. Iterative Synthesis and Properties of Cross-Conjugated iso-Polydiacetylene Oligomers. *J. Am. Chem. Soc.* **1999**, *121*, 458−459.
(19) Zhao, Y. M.; Campbell, K.; Tykwinski, R. R. Iterative synthesis and characterization of cross-conjugated iso-polydiacetylenes. *J. Org. Chem.* **2002**, *67*, 336−344.
(20) Zhao, Y. M.; Slepkov, A. D.; Akoto, C. O.; McDonald, R.; Hegmann, F. A.; Tykwinski, R. R. Synthesis, structure, and nonlinear optical properties of cross-conjugated perphenylated iso-polydiacetylenes. *Chem. - Eur. J.* **2005**, *11*, 321−329.
(21) Zhao, Y. M.; Zhou, N. Z.; Slepkov, A. D.; Ciulei, S. C.; McDonald, R.; Hegmann, F. A.; Tykwinski, R. R. Donor/acceptor effects on the linear and nonlinear optical properties of geminal diethynylethenes (g-DEEs). *Helv. Chim. Acta* **2007**, *90*, 909−927.
(22) Nauroozi, D.; Bruhn, C.; Faust, R. Diethynyldiazafluoren-9-ylidene as a π Cross-Conjugated Platform for Redox Active Transition Metal Fragments. *Organometallics* **2019**, DOI: 10.1021/acs.organomet.9b00232.
(23) Xu, G.-L.; Xi, B.; Updegraff, J. B.; Protasiewicz, J. D.; Ren, T. 1,6-Bis(ferrocenyl)-1,3,5-hexatriyne: Novel Preparation and Structural Study. *Organometallics* **2006**, *25*, 5213−5215.
(24) Forrest, W. P.; Cao, Z.; Hassell, K. M.; Prentice, B. M.; Fanwick, P. E.; Ren, T. Diruthenium(III,III) Bis(alkynyl) Compounds with Donor/Acceptor-Substituted geminal-Diethynylethene Ligands. *Inorg. Chem.* **2012**, *51*, 3261−3269.
(25) Forrest, W. P.; Choudhuri, M. M. R.; Kilyanek, S. M.; Natoli, S. N.; Prentice, B. M.; Fanwick, P. E.; Crutchley, R. J.; Ren, T. Synthesis and Electronic Structure of Ru2(Xap)4(Y-gem-DEE) Type Compounds: Effect of Cross-Conjugation. *Inorg. Chem.* **2015**, *54*, 7645−7652.
(26) Bruce, M. I.; Burgun, A.; Fox, M. A.; Jevric, M.; Low, P. J.; Nicholson, B. K.; Parker, C. R.; Skelton, B. W.; White, A. H.; Zaitseva, N. N. Some Ruthenium Derivatives of Penta-1,4-diyn-3-one. *Organometallics* **2013**, *32*, 3286−3299.
(27) Fan, Y.; Li, H.-M.; Zou, G.-D.; Zhang, X.; Pan, Y.-L.; Cao, K.-K.; Zhang, M.-L.; Ma, P.-L.; Lu, H.-T. Diferrocenes Bridged by a Geminal Diethynylethene Scaffold with Varying Pendant Substituents: Electronic Interactions in Cross-Conjugated System. *Organometallics* **2017**, *36*, 4278−4286.
(28) Fan, Y.; Li, H. M.; Zou, G. D.; Zhang, X.; Li, M.; Wu, J. H.; Lu, H. T. Long-distance electronic coupling in diferrocenyl compounds with cross-conjugated germinal-diethynylethene bridges. *J. Organomet. Chem.* **2018**, *859*, 99−105.
(29) Vincent, K. B.; Gluyas, J. B. G.; Zeng, Q.; Yufit, D. S.; Howard, J. A. K.; Hartl, F.; Low, P. J. Sandwich and half-sandwich metal complexes derived from cross-conjugated 3-methylene-penta-1,4-diynes. *Dalton Trans.* **2017**, *46*, 5522−5531.
(30) Makhoul, R.; Gluyas, J. B. G.; Vincent, K. B.; Sahnoune, H.; Halet, J. F.; Low, P. J.; Hamon, J. R.; Lapinte, C. Redox Properties of Ferrocenyl Ene-diynyl-Bridged Cp*(dppe)M-C C-1,4-(C6H4) Complexes. *Organometallics* **2018**, *37*, 4156−4171.
(31) Tatebe, C. J.; Kiernicki, J. J.; Higgins, R. F.; Ward, R. J.; Natoli, S. N.; Langford, J. C.; Clark, C. L.; Zeller, M.; Wenthold, P.; Shores, M. P.; Walensky, J. R.; Bart, S. C. Investigation of the Electronic Structure of Aryl-Bridged Dinuclear U(III) and U(IV) Compounds. *Organometallics* **2019**, *38*, 1031−1040.
(32) Gao, H.; Mallick, S.; Cao, L.; Meng, M.; Cheng, T.; Chen, H. W.; Liu, C. Y. Electronic Coupling and Electron Transfer between Two Mo2 Units through meta- and para-Phenylene Bridges. *Chem. - Eur. J.* **2019**, *25*, 3930−3938.
(33) Ren, T. A Sustainable Metal Alkynyl Chemistry: 3d Metals and Polyaza Macrocyclic Ligands. *Chem. Commun.* **2016**, *52*, 3271−3279.
(34) Banziger, S. D.; Ren, T. Syntheses, Structures and Bonding of 3d Metal Alkynyl Complexes of Cyclam and Its Derivatives. *J. Organomet. Chem.* **2019**, *885*, 39−48.
(35) Cao, Z.; Forrest, W. P.; Gao, Y.; Fanwick, P. E.; Ren, T. trans-[Fe(cyclam)(C2R)2]+: A New Family of Fe(III) Bis-Alkynyl Compounds. *Organometallics* **2012**, *31*, 6199−6206.
(36) Cao, Z.; Fanwick, P. E.; Forrest, W. P.; Gao, Y.; Ren, T. New Fe(III)(cyclam) Complexes Bearing Axially Bound geminal-Diethynylethenes. *Organometallics* **2013**, *32*, 4684−4689.
(37) Natoli, S. N.; Cook, T. D.; Abraham, T. R.; Kiernicki, J. J.; Fanwick, P. E.; Ren, T. Cobalt(III) Bridged by gem-DEE: Facile Access to A New Class of Cross-Conjugated Organometallics. *Organometallics* **2015**, *34*, 5207−5209.
(38) Natoli, S. N.; Azbell, T. J.; Fanwick, P. E.; Zeller, M.; Ren, T. A Synthetic Approach to Cross-pi-Conjugated Organometallic Systems Based on geminal-Diethynylethene and CoIII(cyclam). *Organometallics* **2016**, *35*, 3594−3603.
(39) Zhao, Y.; McDonald, R.; Tykwinski, R. R. Synthesis and characterization of cross-conjugated polyenynes. *Chem. Commun.* **2000**, 77−78.

DOI: 10.1021/acs.organomet.9b00313
Organometallics 2019, 38, 2758−2769

(40) Cook, T. D.; Natoli, S. N.; Fanwick, P. E.; Ren, T. Co-III(cyclam) Oligoynyls: Monomeric Oligoynyl Complexes and Dimeric Complexes with an Oligoyn-diyl Bridge. *Organometallics* **2016**, *35*, 1329−1338.
(41) Natoli, S. N.; Zeller, M.; Ren, T. Diruthenium-DMBA compounds bearing extended cross-conjugated ligands. *J. Organomet. Chem.* **2017**, *847*, 90−96.
(42) Hay, A. S. Oxidative Coupling of Acetylenes. II1. *J. Org. Chem.* **1962**, *27*, 3320−3321.
(43) Haque, A.; Al-Balushi, R. A.; Al-Busaidi, I. J.; Khan, M. S.; Raithby, P. R. Rise of Conjugated Poly-ynes and Poly(Metalla-ynes): From Design Through Synthesis to Structure-Property Relationships and Applications. *Chem. Rev.* **2018**, *118*, 8474−8597.
(44) Natoli, S. N.; Azbell, T. J.; Fanwick, P. E.; Zeller, M.; Ren, T. A Synthetic Approach to Cross-Conjugated Organometallic Complexes Based on geminal-Diethynylethene and CoIII(cyclam). *Organometallics* **2016**, *35*, 3594−3603.
(45) Zhao, Y.; McDonald, R.; Tykwinski, R. R. Study of Cross-Conjugated iso-Polytriacetylenes and Related Oligoenynes. *J. Org. Chem.* **2002**, *67*, 2805−2812.
(46) Tanimoto, H.; Fujiwara, T.; Mori, J.; Nagao, T.; Nishiyama, Y.; Morimoto, T.; Ito, S.; Tanaka, K.; Chujo, Y.; Kakiuchi, K. Extended germa[N]pericyclynes: synthesis and characterization. *Dalton Trans.* **2017**, *46*, 2281−2288.
(47) Natoli, S. N.; Cook, T. D.; Abraham, T. R.; Kiernicki, J. J.; Fanwick, P. E.; Ren, T. Cobalt(III) Bridged by gem-DEE: Facile Access to a New Type of Cross-Conjugated Organometallics. *Organometallics* **2015**, *34*, 5207−5209.
(48) Cook, T. D.; Natoli, S. N.; Fanwick, P. E.; Ren, T. Dimeric Complexes of CoIII(cyclam) with a Polyynediyl Bridge. *Organometallics* **2015**, *34*, 686−689.
(49) Frisch, M. J.; Trucks, G. W.; Schlegel, H. B.; Scuseria, G. E.; Robb, M. A.; Cheeseman, J. R.; Scalmani, G.; Barone, V.; Petersson, G. A.; Nakatsuji, H.; Li, X.; Caricato, M.; Marenich, A. V.; Bloino, J.; Janesko, B. G.; Gomperts, R.; Mennucci, B.; Hratchian, H. P.; Ortiz, J. V.; Izmaylov, A. F.; Sonnenberg, J. L.; Williams-Young, D.; Ding, F.; Lipparini, F.; Egidi, F.; Goings, J.; Peng, B.; Petrone, A.; Henderson, T.; Ranasinghe, D.; Zakrzewski, V. G.; Gao, J.; Rega, N.; Zheng, G.; Liang, W.; Hada, M.; Ehara, M.; Toyota, K.; Fukuda, R.; Hasegawa, J.; Ishida, M.; Nakajima, T.; Honda, Y.; Kitao, O.; Nakai, H.; Vreven, T.; Throssell, K.; Montgomery, J. A., Jr.; Peralta, J. E.; Ogliaro, F.; Bearpark, M. J.; Heyd, J. J.; Brothers, E. N.; Kudin, K. N.; Staroverov, V. N.; Keith, T. A.; Kobayashi, R.; Normand, J.; Raghavachari, K.; Rendell, A. P.; Burant, J. C.; Iyengar, S. S.; Tomasi, J.; Cossi, M.; Millam, J. M.; Klene, M.; Adamo, C.; Cammi, R.; Ochterski, J. W.; Martin, R. L.; Morokuma, K.; Farkas, O.; Foresman, J. B.; Fox, D. J. *Gaussian 16*, Revision B.01; Gaussian, Inc.: Wallingford, CT, 2016.
(50) Ren, T. Diruthenium 5-Alkynyl Compounds: A New Class of Conjugated Organometallics. *Organometallics* **2005**, *24*, 4854−4870.
(51) Bruschi, M.; Giuffreda, M. G.; Luthi, H. P. trans versus geminal electron delocalization in tetra- and diethynylethenes: A new method of analysis. *Chem. - Eur. J.* **2002**, *8*, 4216−4227.
(52) Limacher, P. A.; Luthi, H. P. Cross-Conjugation. *WIREs Comput. Mol. Sci.* **2011**, *1*, 477−486.
(53) Cao, Z.; Ren, T. DFT Study of Electronic Properties of 3d Metal Complexes of sigma-Geminal Diethynylethenes (*gem*-DEEs). *Organometallics* **2011**, *30*, 245−250.
(54) Bosnich, B.; Poon, C. K.; Tobe, M. L. Complexes of Cobalt(3) with a Cyclic Tetradentate Secondary Amine. *Inorg. Chem.* **1965**, *4*, 1102−1108.
(55) Beurskens, P. T.; Beurskens, G.; de Gelder, R.; Garcia-Granda, S.; Gould, R. O.; Smits, J. M. M. *DIRDIF2008 Program. The DIRDIF2008 Program System*; Crystallography Laboratory, Univeristy of Nijmegen: The Netherlands, 2008.
(56) Bruker Advanced X-ray Solutions, *SHELXTL Suite of Programs*; Bruker AXS Inc.: Madison, WI, 2003.

DOI: 10.1021/acs.organomet.9b00313
Organometallics 2019, 38, 2758−2769